Interaction induced edge channel equilibration

Anders Mathias Lunde,* Simon E. Nigg, and Markus Büttiker
Département de Physique Théorique, Université de Genève, CH-1211 Genève 4, Switzerland
(Dated: October 14, 2009)

The electronic distribution functions of two Coulomb coupled chiral edge states forming a quasi-1D system with broken translation invariance are found using the equation of motion approach. We find that relaxation and thereby energy exchange between the two edge states is determined by the shot noise of the edge states generated at a quantum point contact (QPC). In close vicinity to the QPC, we derive analytic expressions for the distribution functions. We further give an iterative procedure with which we can compute numerically the distribution functions arbitrarily far away from the QPC. Our results are compared with recent experiments of Le Sueur et al..

PACS numbers: 73.23.-b, 73.43.Cd, 72.70.+m

Two decades ago, edge states (ES's) [1] were demonstrated to be a physical reality by creating a non-equilibrium population [2] through selective injection and detection of carriers in different states along the same edge [3, 4, 5]. Experiments revealed that the inter-edge carrier scattering could be strongly suppressed [3, 4, 5] over distances of 80 μm. Now in a series of novel experiments the group of Pierre [6, 7] has investigated the non-equilibrium distribution function in an ES as it evolves along a channel away from a QPC at which it is initially created. The experiments are carried out in a high mobility two-dimensional electron gas at a filling factor $\nu = 2$ such that there is an outer (spin up) non-equilibrium ES and an inner (spin down) equilibrium ES. The distribution function is measured with the help of a quantum dot (QD) sufficiently small to provide transmission only through a single resonant level, see fig. 1. The QD serves as an energy spectrometer and permits the reconstruction of the distribution function in the outer ES.

The experiments reveal two surprising features: First, the initial non-equilibrium distribution created at the QPC and calculated form non-interacting scattering theory differs only weakly from the measured one over distances of close to one micrometer [6, 7]. At large distances from the QPC, due to the Coulomb interaction between carriers in the two ES's, the distribution function evolves into an equilibrium distribution function at an effective electrochemical potential and temperature. The outer non-equilibrium ES transfers part of its energy to the inner ES. The two ES's equilibrate towards the same equilibrium distribution with the same temperature (but still at different electrochemical potentials due to lack of particle exchange between the two ES's). The second surprise of the experiments is the fact that the temperature of the distribution functions at large distance in the two ES's is *lower* than dictated by equilibrium thermodynamic arguments [7]. The first surprise shows that relaxation due to inter-ES interaction is weak. The second surprise implies that equilibration occurs not only between the inner and outer ES's but that there must be an additional equilibration mechanism which cools the two ES's below what would be expected from inter-ES coupling alone. We propose that additional excitations in the bulk [8], which couple predominantly to the inner ES, have to be considered to understand this effect. Although the nature of these excitations remains unclear, the experimental findings of [7] are consistent with this hypothesis. For example it is found that when the inner ES is forced to form a short closed loop, then relaxation in the outer ES is strongly suppressed.

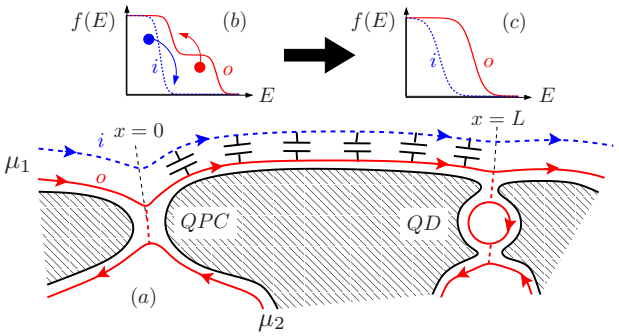

FIG. 1: (color online). (a) The experimental setup to measure the electronic distribution function of an ES. The full (red) curve represents the measured outer ES while the dashed (blue) curve represents a co-propagating inner ES. The two ES's exchange energy via Coulomb interaction between $x = 0$ and $x = L$. The initial distribution functions (b) relax, via energy-conserving particle-hole excitation processes, toward Fermi functions (c).

The physics of ES's is often discussed within the framework of bosonization theory, where the elementary excitations have bosonic character and are of collective nature [9, 10]. In contrast, we take the weak equilibration seen at distances of less than a micrometer as the starting point of a discussion which treats inter-ES interaction perturbatively [11]. The interaction is described in terms of two-body collisions. We use the equation of motion approach for second quantized operators to derive an evolution equation for the distribution functions which resembles a Boltzmann collision term with the added complication that there are two different initial distributions

(one for each ES). Alternatively the Coulomb matrix elements which appear in this theory can be taken from an RPA theory [12] in which the electron densities in each channel fluctuate and interact through an (effective) capacitance. To treat equilibration at longer distances we iterate numerically the solution for short distances. At large distances the distribution functions approach their equilibrium form dictated by entropy maximization.

We describe the ES's in terms of scattering states $\chi_{\alpha E}(x)$ with energy E and label $\alpha = o, i$ (i : inner, o : outer). The inter-ES interaction is given by

$$H_{\rm int} = \frac{1}{2}\sum_{\alpha}\int \mathrm{d}E\,\mathrm{d}E'\,U_\alpha(E',E)\,a^\dagger_{\alpha E'}a_{\alpha E}, \qquad (1)$$

where $a^\dagger_{\alpha E}$ ($a_{\alpha E}$) is the creation (annihilation) operator for the scattering state $\chi_{\alpha E}$ and $U_\alpha(E',E)$ is the potential operator for scattering a particle from E to E' in the ES α at the expense of a particle scattering in the opposite ES $\bar\alpha$. Explicitly $U_\alpha(E_{1'},E_1,t) = \int \mathrm{d}E_2\mathrm{d}E_{2'}V^{\alpha\bar\alpha}_{E_{1'}E_{2'},E_1E_2}a^\dagger_{\bar\alpha E_{2'}}(t)a_{\bar\alpha E_2}(t)$ in the Heisenberg picture and $V^{\alpha\bar\alpha}_{E_{1'}E_{2'},E_1E_2}$ is the inter-ES electron-electron interaction matrix element for the scattering process $(\alpha E_1,\bar\alpha E_2)\to(\alpha E_{1'},\bar\alpha E_{2'})$. Using the Heisenberg equation of motion $i\hbar\partial_t a_{\alpha E}(t) = [a_{\alpha E}(t), H]$, the electronic distribution function $f_\alpha(E)$ in ES α can be found by evaluating $\langle a^\dagger_{\alpha E}(t)a_{\alpha E'}(t)\rangle = \delta(E-E')f_\alpha(E)$. The non-interacting distributions are $f^0_i(E) = f^0_{\mu_i}(E)$ and $f^0_o(E) = \mathcal{R}f^0_{\mu_1}(E) + \mathcal{T}f^0_{\mu_2}(E)$, where $f^0_\mu \equiv \{1+\exp[(E-\mu)/k_{\rm B}T]\}^{-1}$ and $\mathcal{T}$ ($\mathcal{R}$) is the transmission (reflection) probability of the QPC, see Fig. 1. The chemical potential of the inner ES μ_i can experimentally be tuned independently of μ_1 and μ_2 by using an additional QPC (not shown in Fig. 1). To second order in the interaction matrix element the distribution is $f^{(2)}_\alpha = f^0_\alpha + \delta f^{(2)}_\alpha$, where (see Supplementary Material for details)

$$\delta f^{(2)}_\alpha(E) = 2\pi\int_{-\infty}^{\infty}\mathrm{d}\omega\Big[f^0_\alpha(E+\hbar\omega)[1-f^0_\alpha(E)]S^a_{\delta U_\alpha\delta U_\alpha}(E,E+\hbar\omega,\omega) - f^0_\alpha(E)[1-f^0_\alpha(E+\hbar\omega)]S^e_{\delta U_\alpha\delta U_\alpha}(E+\hbar\omega,E,\omega)\Big]. \qquad (2)$$

The first term contains the absorption potential fluctuation spectrum [13] $S^a_{\delta U_\alpha\delta U_\alpha}(E,E',\omega)$ describing an absorption of energy $\hbar\omega$ by the ES $\bar\alpha$ while the ES α goes from energy E' to E. Likewise the second term with the emission fluctuation spectrum $S^e_{\delta U_\alpha\delta U_\alpha}$ describes the emission of energy $\hbar\omega$ from the ES $\bar\alpha$ to the ES α, which consequently leads to the transition $E\to E+\hbar\omega$ in α. The fluctuation spectra are to lowest order in the interaction and defined by $2\pi\delta(\omega+\omega')S^a_{\delta U_\alpha\delta U_\alpha}(E',E,\omega) \equiv \langle\delta U_\alpha(E,E',\omega)^{(1)}\delta U_\alpha(E',E,\omega')^{(1)}\rangle$, where $\delta U^{(1)}_\alpha \equiv U^{(1)}_\alpha - \langle U^{(1)}_\alpha\rangle$ is the Fourier transformed operator for the deviation from the average potential to first order in the interaction. The emission spectrum is found by interchanging the two δU_α in the absorption spectrum or equivalently by changing the sign of ω. Explicitly, the spectra are found to be

$$S^a_{\delta U_\alpha\delta U_\alpha}(E',E,\omega) = h\int\mathrm{d}E''|V^{\alpha\bar\alpha}_{E'E''+\hbar\omega,EE''}|^2 f^0_\alpha(E'')[1-f^0_{\bar\alpha}(E''+\hbar\omega)], \qquad (3a)$$

$$S^e_{\delta U_\alpha\delta U_\alpha}(E',E,\omega) = h\int\mathrm{d}E''|V^{\alpha\bar\alpha}_{E'E'',EE''+\hbar\omega}|^2 f^0_\alpha(E''+\hbar\omega)[1-f^0_{\bar\alpha}(E'')], \qquad (3b)$$

where the interpretation in terms of emission and absorption spectra is clear. By inserting these into Eq. (2) the similarity with the collision integral in the Boltzmann equation becomes evident.

Next we wish to calculate $\delta f^{(2)}_\alpha(E)$. To this end, the inter-ES scattering process $(\alpha E_1,\bar\alpha E_2)\to(\alpha E_{1'},\bar\alpha E_{2'})$ needs to be considered. If the ES's are perfectly translation invariant, then energy *and* momentum conservation together reduce the available one dimensional phase space enormously compared to higher dimensions [14]. This leads us to consider the more realistic non-translation invariant case caused by the fact that the ES's follow the equipotential lines created by the sample edges and the impurity potential. Including this non-translation invariant ES physics leads to the presence of non-momentum conserving scattering processes increasing the phase space substantially [15, 16]. The broken translation invariance is included into the model of the inter-ES interaction matrix element $|V^{\alpha\bar\alpha}_{E_{1'}E_{2'},E_1E_2}|^2$. To avoid modeling a specific geometry we perform a statistical average over the geometry of the ES's and thereby introduce the momentum breaking correlation length ℓ_p, which is smaller than the size of the region of relaxation L. For simplicity, an effective interaction of the form $V(x,x') = \delta(x-x')g(x)$ is used and it is assumed that the deviation of $g(x)$ from some mean value g_0 is Gaussian distributed, i.e. $\overline{(g(x)-g_0)(g(x')-g_0)} = A/(\sqrt{2\pi}\ell_p)\exp\big[-(x-x')^2/(2\ell_p^2)\big]$ where $A/(\sqrt{2\pi}\ell_p)$ is the maximal deviation and $\overline{\cdots}$ denotes the geometrical averaging. This yields an interaction with a momentum conserving and a momentum breaking part. The latter is (see Supplementary Material for details)

$$\overline{|V^{\alpha\bar\alpha}_{E_{1'}E_{2'},E_1E_2}|^2}_{\Delta k\neq 0} = \frac{AL}{h^4v_\alpha^2v_{\bar\alpha}^2}\exp\big[-(\Delta k\ell_p)^2/2\big], \qquad (4)$$

where $\Delta k = (E_1-E_{1'})/(\hbar v_\alpha) + (E_2-E_{2'})/(\hbar v_{\bar\alpha})$, using linear dispersion relations with different velocities v_α for the two ES's. Note that for linear dispersions with *different* velocities there is no phase space for scattering in the momentum conserving limit, $\Delta k = 0$, but in the very special (almost pathological) case $v_\alpha = v_{\bar\alpha}$, momentum and energy conservation are equivalent leading to plenty

of phase space. The specific model for the interaction and the matrix element is not of great importance as long as it includes the physics leading to non-momentum conserving processes, which in turn introduces a new length scale ℓ_p.

For energy conserving scattering, the model matrix element Eq. (4) only depends on the transferred energy in the scattering [17], since $\Delta k = \omega(1/v_\alpha - 1/v_{\bar\alpha})$. This means that the energy integral in the fluctuation spectra of Eqs. (3) can be done analytically upon which it becomes evident that $\delta f_\alpha^{(2)}(E) \propto \mathcal{T}(1-\mathcal{T})$. Thus the greater the shot noise of the QPC, the faster the relaxation is. The elementary scattering processes leading to relaxation consist of a particle loosing energy in the noisy outer ES and a particle gaining energy in the noiseless inner ES as illustrated on Fig. 1, (b). The matrix element introduces a new energy scale $\Delta E \equiv (\hbar/\ell_p)v_\alpha v_{\bar\alpha}/(v_{\bar\alpha} - v_\alpha)$, which limits the possible amount of energy transferred between the two ES's in the scattering process since the matrix element is proportional to $e^{-(\hbar\omega/\Delta E)^2}$. In the limit that $k_{\rm B}T, |\mu_2 - \mu_1| \ll |\Delta E|$ the distribution functions for the inner and outer ES can be found analytically to be

$$\delta f_o^{(2)}(E) = -\gamma^2\mathcal{T}(1-\mathcal{T})(\mu_2-\mu_1) \times [f^0_{\mu_2}(E) - f^0_{\mu_1}(E)]\Big[E - \frac{1}{2}(\mu_1+\mu_2)\Big], \quad (5)$$

$$\delta f_i^{(2)}(E) = \frac{\gamma^2}{2}\mathcal{T}(1-\mathcal{T}) \times\Big\{ -[f^0_{\mu_i}(E) - f^0_{\mu_i^-}(E)]\big[(\pi k_{\rm B}T)^2 + (E-\mu_i^-)^2\big] + [f^0_{\mu_i^+}(E) - f^0_{\mu_i}(E)]\big[(\pi k_{\rm B}T)^2 + (E-\mu_i^+)^2\big]\Big\}, \quad (6)$$

where $\gamma^2 \equiv (2\pi)^2 AL/[h^4 v_\alpha^2 v_{\bar\alpha}^2]$ and $\mu_i^\pm = \mu_i \pm (\mu_2 - \mu_1)$ is the maximal and minimal energy of particles affected by the scattering process in the inner ES. Here it is seen that the maximal available energy (apart from thermal excitations of order $k_{\rm B}T$) is given by the energy difference $\mu_2 - \mu_1$ creating the step distribution. The scattering processes create a linear slope on the plateau of the distribution of the noisy outer ES as shown in Fig.2. The slope crosses the middle of the plateau and it is proportional to the noise of the QPC and the energy available $\mu_2 - \mu_1$. The inner noiseless distribution gets a tail on both sides of the Fermi level, which extends over the length of the plateau $\mu_2 - \mu_1$. In the general case, the distribution functions can be found numerically and the matrix elements in Eq. (4) have to be included in the calculation, but the transferred energy is still limited by ΔE.

The above perturbative results apply for a short distance L after the QPC and express the distribution functions at L in terms of the (unperturbed) distribution functions at the origin. Once the distribution functions

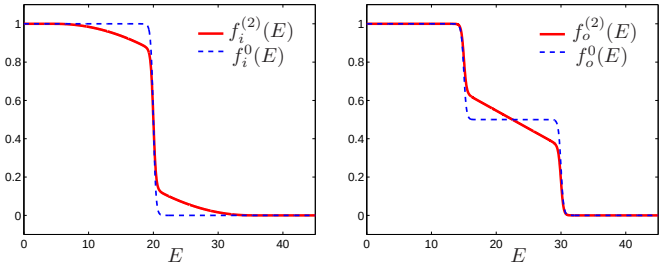

FIG. 2: (color online). Analytically calculated inner (left) and outer (right) ES distribution functions in the regime $k_{\rm B}T, |\mu_2 - \mu_1| \ll |\Delta E|$. The parameters are (energies in μeV): $\mathcal{T} = 0.5$, $\mu_1 = 15$, $\mu_2 = 30$, $\mu_i = 20$, $k_{\rm B}T = 0.2$.

at L are known we can use them to calculate the distribution functions at a distance $2L$ via Eq. (2). By iterating this procedure we can thus describe the effective length dependence of the energy relaxation. A convenient quantity with which to characterize the relaxation of f_α at temperature T is given by the *excess temperature* $T_{exc,\alpha}$ [6] defined as

$$k_{\rm B}T_{exc,\alpha} \equiv \sqrt{\frac{6}{\pi^2}\int {\rm d}E \Delta f_\alpha(E)(E - \tilde\mu_\alpha) - (k_{\rm B}T)^2}\,. \quad (7)$$

Here $\Delta f_\alpha(E) = f_\alpha(E) - \theta(\tilde\mu_\alpha - E)$ is the difference between the actual distribution function and a zero temperature Fermi distribution with the same number of particles and hence $\tilde\mu_\alpha = E_0 + \int_{E_0}^\infty {\rm d}E f_\alpha(E)$, where E_0 is chosen such that $f_\alpha(E) = 1$ for $E < E_0$. $k_{\rm B}T_{exc,\alpha}$ gives the energy of the non-thermal excitations in f_α. The initial excess temperature right after the QPC of the inner ES is zero and the one of the outer ES is given by $k_{\rm B}T^0_{exc,o} = \{\frac{3}{\pi^2}\mathcal{T}(1-\mathcal{T})\}^{1/2}|\mu_2 - \mu_1|$. Because of energy conservation, $\sum_\alpha T_{exc,\alpha}$ is a conserved quantity in the equilibration process. Furthermore due to entropy maximization the excess energy is distributed equally among the two ES's, which in the limit of long distances thus converge towards Fermi distributions with equal excess temperatures given by $k_{\rm B}T^{\infty(2)}_{exc} = \{\frac{3}{2\pi^2}\mathcal{T}(1-\mathcal{T})\}^{1/2}|\mu_2 - \mu_1|$. The excess temperature of the outer ES measured in [7] does indeed saturate at large distances toward a finite value. This value is however found to be systematically lower than the above prediction, for large voltage biases. Surprisingly it agrees well with the value $k_{\rm B}T^{\infty(3)}_{exc} = \{\mathcal{T}(1-\mathcal{T})\}^{1/2}|\mu_2 - \mu_1|/\pi$ expected from energy equipartition among *three* instead of only two channels. What could provide the additional relaxation channel? In [7] it has been observed that if the inner ES is forced to form a short enough closed loop, such that the energy level spacing of its (discrete) spectrum is larger than the available energy provided by the voltage bias $\mu_2 - \mu_1$, then relaxation of the outer ES is strongly suppressed. Motivated by this observation, we suggest that there exist excitations in the bulk [8], which are coupled

via long range Coulomb interaction to both the inner ES and an ES on the opposite side of the sample. As long as the bulk excitations can be created, such a mechanism would allow extra energy to be carried away from the outer ES.

As a first approach we model this extra degree of freedom as an additional ES coupled to the inner ES only, initially in equilibrium at the electronic temperature, which we take to be $T = 30\,\mathrm{mK}$. This then contributes an extra collision term in Eq. (2) and allows a quantitative comparison with the experiment [7]. The fitting procedure is detailed in Supplementary Material and the result is shown in Fig. 3. The best fit is obtained when the coupling strength to the bulk excitations is about three times larger than the inter-ES coupling strength and when $\Delta E = 14.3\,\mu\mathrm{eV}$, which for v_o and v_i between 10^4 and $10^5\,\mathrm{m/s}$ leads to $\ell_p \geq 0.5\,\mu\mathrm{m}$. For intermediate distances (i.e. $2.2\,\mu\mathrm{m}$ and $4\,\mu\mathrm{m}$) both the data and our numerics display a similar weakly non-linear behavior of the excess temperature as a function of the voltage bias.

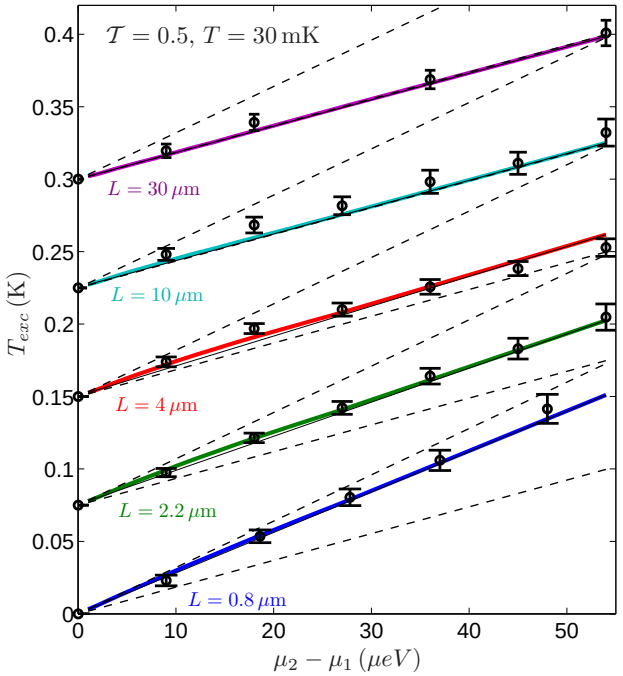

FIG. 3: (color online). The excess temperature of the outer ES versus the voltage difference across the QPC. For clarity curves for different voltages have been shifted upward by 75 mK. The dashed (black) lines indicate the initial value $T^0_{exc,o}$ (upper lines) and the asymptotic value $T^{\infty(3)}_{exc}$ (lower lines) as expected from energy equipartition. The thin (black) lines are guides for the eyes to better see the weak non-linearity present at intermediate distances (especially for $2.2\,\mu\mathrm{m}$ and $4\,\mu\mathrm{m}$). Experimental data (circles with error bars), courtesy of F. Pierre et al..

To conclude, we have computed the distribution functions of two Coulomb-coupled ES's in the integer quantum Hall regime. We derived an analytic expression for the leading order correction to the non-interacting theory, which is present in a system without translation invariance. We have shown further that the result obtained in the long distance limit, by iterating the perturbative solution numerically, is in quantitative agreement with a recently performed experiment if we take into account the electric coupling between the innermost ES and bulk excitations. Finally we note that measurements of the distribution functions of both channels for even shorter distances than $0.8\,\mu\mathrm{m}$ should allow for further critical testing of our theory.

The authors would like to thank H. Le Sueur, C. Altimiras and F. Pierre for fruitful discussion and for sharing their data. This work was supported by the Swiss NSF.

Note added.—During completion of this work we became aware of related work based on plasmon scattering by P. Degiovanni et al. [10].

* Corresponding author: mathias.lunde@unige.ch

[1] B. I. Halperin, Phys. Rev. B **25**, 2185 (1982).
[2] M. Büttiker, Phys. Rev. B **38**, 9375 (1988).
[3] S. Komiyama, H. Hirai, S. Sasa, and S. Hiyamizu, Phys. Rev. B **40**, 12566 (1989).
[4] B. J. van Wees, E. M. M. Willems, C. J. P. M. Harmans, C. W. J. Beenakker, H. van Houten, J. G. Williamson, C. T. Foxon, and J. J. Harris, Phys. Rev. Lett. **62**, 1181 (1989).
[5] B. W. Alphenaar, P. L. McEuen, R. G. Wheeler, and R. N. Sacks, Phys. Rev. Lett. **64**, 677 (1990).
[6] C. Altimiras, H. le Sueur, U. Gennser, A. Cavanna, D. Mailly, and F. Pierre, Nat. Phys. (2009), (unpublished).
[7] H. le Sueur, C. Altimiras, U. Gennser, A. Cavanna, D. Mailly, and F. Pierre (2009), (unpublished).
[8] G. Granger, J. P. Eisenstein, and J. L. Reno, Phys. Rev. Lett. **102**, 086803 (2009).
[9] I. P. Levkivskyi and E. V. Sukhorukov, Phys. Rev. Lett. **103**, 036801 (2009); D. L. Kovrizhin and J. T. Chalker, e-print arXiv:0903.3387.
[10] P. Degiovanni, C. Grenier, G. Fève, C. Altimiras, H. le Sueur, and F. Pierre (2009), (unpublished).
[11] When the available energy $eV \leq \hbar\omega_p = \hbar v_F/gL$ where ω_p is the lowest plasma mode frequency in the system, collective modes are not excited and electron transport appears effectively to be non-interacting. Here v_F is the Fermi velocity, g is the Luttinger interaction parameter, and L the length of the conductor. See Refs. [12]. Distribution functions in Carbon nanotubes also deviate only weakly from non-interacting theory, see Yung-Fu Chen et al., Phys. Rev. Lett. **102**, 036804 (2009) and C. Bena, e-print arXiv:0909.0867.
[12] Y. M. Blanter, F. W. J. Hekking, and M. Büttiker, Phys. Rev. Lett. **81**, 1925 (1998); A. M. Martin and M. Büttiker, Phys. Rev. Lett. **84**, 3386 (2000); P. Roulleau, F. Portier, P. Roche, A. Cavanna, G. Faini, U. Gennser, and D. Mailly, Phys. Rev. Lett. **101**, 186803 (2008).

[13] R. Aguado and L. P. Kouwenhoven, Phys. Rev. Lett. **84**, 1986 (2000).
[14] A. M. Lunde, K. Flensberg, and L. I. Glazman, Phys. Rev. Lett. **97**, 256802 (2006) and Phys. Rev. B **75**, 245418 (2007).
[15] J. Rech and K. A. Matveev, Phys. Rev. Lett. **100**, 066407 (2008).
[16] A. M. Lunde, A. D. Martino, A. Schulz, R. Egger, and K. Flensberg, New. J. Phys. **11**, 023031 (2009).
[17] This is a common feature of most models of the matrix elements.
[18] C. W. J. Beenakker and H. van Houten, Solid State Phys. **44**, 1 (1991).
[19] H. Pothier, S. Guéron, N. O. Birge, D. Esteve, and M. H. Devoret, Phys. Rev. Lett. **79**, 3490 (1997).
[20] D. T. McClure, Y. Zhang, B. Rosenow, E. M. Levenson-Falk, C. M. Marcus, L. N. Pfeiffer, and K. W. West (2009), e-print arxiv:0903.5097v1.

Supplementary Material for "Interaction induced edge channel equilibration"

In this Supplementary Material we present details of the derivation of the leading order correction to the distribution functions as given in Eq. (2) of the main text. We also describe the model used for the Coulomb matrix elements given in Eq. (4) of the main text. Finally, we explain the iteration procedure and how we fitted our theoretical predictions with the experiment of [7].

THE EQUATION OF MOTION APPROACH AND THE DISTRIBUTION FUNCTION

Our starting point is the Hamiltonian describing the dynamics of the electrons in the inner and outer ES's after the QPC:

$$H = \sum_{\alpha=i,o} \int \mathrm{d}x\, \psi^\dagger_\alpha(x) T^\alpha(x) \psi_\alpha(x) + \frac{1}{2}\sum_{\alpha\beta} \int \mathrm{d}x\, \mathrm{d}x'\, \psi^\dagger_\alpha(x)\psi^\dagger_\beta(x') V_{\alpha\beta}(x,x')\psi_\beta(x')\psi_\alpha(x)\,. \tag{8}$$

The first term describes the kinetic energy plus the single particle potential and the second term the *inter* and *intra* ES Coulomb interaction of the outer (o) and inner (i) ES's. The intra-ES interaction typically leads only to a small contribution to the relaxation due to the presence of both the direct and the exchange term as we shall see shortly. Therefore the focus in the paper is on the inter-ES interaction $V_{\alpha\bar\alpha}$, using the shorthand notation $\bar\alpha = \delta_{i\alpha}o + \delta_{o\alpha}i$ (for the opposite ES of α). Introducing the scattering state representation

$$a_{\alpha E} = \int \mathrm{d}x\, \chi^*_{\alpha E}(x)\psi_\alpha(x) \quad \Leftrightarrow \quad \psi_\alpha(x) = \int \mathrm{d}E\, \chi_{\alpha E}(x) a_\alpha(E)\,, \tag{9}$$

makes the single-particle part of the Hamiltonian diagonal. In this representation, the equation of motion for the annihilation operators $i\hbar\partial_t a_{\alpha E}(t) = [a_{\alpha E}(t), H]$ in the Heisenberg picture (i.e. $A(t) \equiv e^{iHt}Ae^{-iHt}$) becomes

$$i\hbar\frac{\mathrm{d}}{\mathrm{d}t}a_{\alpha E}(t) = E a_{\alpha E}(t) + \int \mathrm{d}E'\, U_\alpha(E,E',t) a_{\alpha E'}(t)\,. \tag{10}$$

In the case of inter-ES interactions only, the potential operator is given by

$$U_\alpha(E,E',t) = \int \mathrm{d}E_2 \mathrm{d}E_{2'} V^{\alpha\bar\alpha}_{EE_{2'},E'E_2} a^\dagger_{\bar\alpha E_{2'}}(t) a_{\bar\alpha E_2}(t)\,, \tag{11}$$

where $V^{\alpha\bar\alpha}_{EE_{2'},E'E_2}$, defined in Eq. (16) below, is the Coulomb matrix element for a transition from an energy E' to E in ES α and a simultaneous transition from energy E_2 to $E_{2'}$ in ES $\bar\alpha$. A standard perturbation treatment to second order in $V^{\alpha\bar\alpha}$ leads to the result

$$\delta(E-E')f^{(2)}_\alpha(E) \equiv \langle a^\dagger_{\alpha E} a_{\alpha E'}\rangle^{(2)} = \delta(E-E')\left(f^0_\alpha(E) + \delta f^{(2)}_\alpha(E)\right)\,, \tag{12}$$

with the inter-ES relaxation given by

$$\begin{aligned}\delta f^{(2)}_\alpha(E) = (2\pi)^2\hbar \int \mathrm{d}\omega\, \mathrm{d}E' |V^{\alpha\bar\alpha}_{EE'+\hbar\omega,E+\hbar\omega E'}|^2 \\ \times \Big[f^0_\alpha(E+\hbar\omega)[1-f^0_\alpha(E)]f^0_{\bar\alpha}(E')[1-f^0_{\bar\alpha}(E'+\hbar\omega)] - f^0_\alpha(E)[1-f^0_\alpha(E+\hbar\omega)]f^0_{\bar\alpha}(E'+\hbar\omega)[1-f^0_{\bar\alpha}(E')]\Big]\,.\end{aligned} \tag{13}$$

The combination of Fermi functions which appears here ensures the Pauli exclusion principle. Furthermore one can easily show that

$$\langle \delta U_\alpha(E,E',\omega)^{(1)} \delta U_\alpha(E',E,\omega')^{(1)}\rangle = (2\pi)^2\hbar\delta(\omega+\omega')\int \mathrm{d}E_{2'} |V^{\alpha\bar\alpha}_{E'E_{2'}+\hbar\omega,EE_{2'}}|^2 f^0_{\bar\alpha}(E_{2'})[1-f^0_{\bar\alpha}(E_{2'}+\hbar\omega)]\,, \tag{14}$$

where $\delta U_\alpha(E,E',\omega)^{(1)} = U_\alpha(E,E',\omega)^{(1)} - \langle U_\alpha(E,E',\omega)^{(1)}\rangle$ and $U_\alpha(E,E',\omega)^{(1)}$ is the Fourier transform of the first order expansion of (11). This then leads immediately to Eq. (2) of the main text.

The relaxation due to intra-ES interactions can be found in the same way. The result is as in Eq. (13) with the important replacement:

$$|V^{\alpha\bar{\alpha}}_{EE'+\hbar\omega,E+\hbar\omega E'}|^2 \to \frac{1}{2}|\underbrace{V^{\alpha\alpha}_{EE'+\hbar\omega,E+\hbar\omega E'}}_{\text{direct term}} - \underbrace{V^{\alpha\alpha}_{E'+\hbar\omega E,E+\hbar\omega E'}}_{\text{exchange term}}|^2, \tag{15}$$

where the two final states were exchanged in the second term called the exchange term. The appearance of both the direct and the exchange interaction is due to the fact that the electrons are in the same conductor and hence quantum mechanical exchange processes are important. For the simple matrix element model used below, the direct and exchange elements exactly cancel. Although this cancellation is model dependent, the intra-ES contribution is strongly suppressed as a general feature and is therefore safely neglected in the present work.

Finally, we note that the generalization to more than two coupled ES's is straightforward and formally results in additional collision terms in Eq. (13). In the following, we make use of this generalization to incorporate the effect of an extra relaxation channel.

MODEL FOR THE COULOMB MATRIX ELEMENTS

The interaction matrix element is

$$V^{\alpha_1\alpha_2}_{E_{1'}E_{2'},E_1E_2} \equiv \int \mathrm{d}x\,\mathrm{d}x' \chi^*_{\alpha_1E_{1'}}(x)\chi^*_{\alpha_2E_{2'}}(x')V_{\alpha_1\alpha_2}(x,x')\chi_{\alpha_2E_2}(x')\chi_{\alpha_1E_1}(x), \tag{16}$$

where $V_{\alpha_1\alpha_2}(x,x')$ is the effective Coulomb interaction between an electron at x in ES α_1 and an electron at x' in ES α_2. In the adiabatic edge channel description [18], ES's follow the equipotential lines in the sample. Due to impurities near the edge and to the variation of the confining potential, the inter-ES distance is not constant in the direction of propagation. In other words, translation invariance is broken and momentum is not conserved in the collision process. For the sake of generality, we do not model a specific geometry nor impurity distribution, but instead simply average over the geometry. This naturally introduces a momentum breaking correlation length scale ℓ_p quantifying the amount of momentum breaking present in the system.

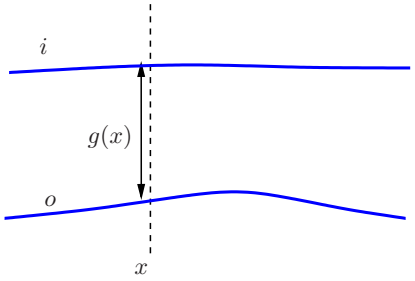

FIG. 4: (color online). Schematics of two co-propagating edge states with varying inter-edge state distance.

As a specific simple example, we consider the interaction between points with the same x coordinate as illustrated in Fig. 4, i.e. $V_{\alpha\bar{\alpha}}(x,x') = \delta(x-x')g(x)$, where $g(x)$ is an unknown function of the interaction strength variation along the ES's. This approximation is justified for very good screening. However, it is important to emphasize [19] that this simplification is not of vital importance for the physics discussed here, i.e. if we consider the poor screening limit, then the same physical effect of the broken translation invariance remains as can be shown from a more complete calculation. We assume linear dispersion relations with constant velocities v_α and use a single particle basis of plane wave states

$$\chi_{\alpha E}(x) = \frac{1}{\sqrt{hv_\alpha}} e^{ik_\alpha(E)x}, \quad \text{with} \quad k_\alpha(E) = \frac{E}{\hbar v_\alpha}. \tag{17}$$

Note that these states are normalized to have equal current and obey $\int \mathrm{d}x \chi^*_{\alpha E}(x)\chi_{\alpha E'}(x) = \delta(E-E')$. With the above assumptions, we obtain

$$V^{\alpha\bar{\alpha}}_{E_{1'}E_{2'},E_1E_2} = \frac{1}{h^2 v_\alpha v_{\bar{\alpha}}} \int_{-L/2}^{L/2} \mathrm{d}x\, e^{i\Delta k x} g(x)\,, \tag{18}$$

where the amount of broken momentum conservation $\Delta k = k_\alpha(E_1) + k_{\bar{\alpha}}(E_2) - k_\alpha(E_{1'}) - k_{\bar{\alpha}}(E_{2'})$ is introduced and x is integrated over the region of relaxation of length L. Next the geometrical averaging of the squared matrix element $|V^{\alpha\bar{\alpha}}_{E_{1'}E_{2'},E_1E_2}|^2$ is performed by assuming that the deviation $\Delta g(x) = g(x) - g_0$ is Gaussian distributed, i.e. $\overline{\Delta g(x)\Delta g(x')} = A/(\sqrt{2\pi}\ell_p)\exp[-(x-x')^2/(2\ell_p^2)]$, as described in the main text. This gives two contributions to $\overline{|V^{\alpha\bar{\alpha}}_{E_{1'}E_{2'},E_1E_2}|^2}$: one with $\Delta k = 0$ and one where $\Delta k \neq 0$ is possible. The latter is given by Eq. (4) of the main text. Note that it is proportional to L, because interaction is included only over a region of length L.

In this work, linear dispersions with different velocities are used, which leaves no phase space for scattering in the momentum conserving case $\Delta k = 0$ due to simultaneous energy and momentum conservation. In general, the dispersions are not linear and this changes the phase space constraints due to momentum conservation in the translation invariant limit. For instance, for a spin-split quadratic dispersion there would only be a single possible final state, where the two initial momenta are simply interchanged. This would lead to a very small resonant-like feature on the plateau of the outer ES distribution function, which could be tuned along the plateau by the chemical potential of the inner ES μ_i. Any dispersion with a positive curvature will lead to the same result. However, this is a very small increase of the phase space compared to the increase introduced by the non-translation invariant physics and importantly, this is *not* what is observed experimentally. Therefore for the non-translation invariant physics the curvature of the dispersion is without importance and for simplicity the dispersion is linearized.

NUMERICAL ITERATION PROCEDURE

Eqs. (2) and (3a-b) of the main text express the variation of the distribution functions of the ES's after a short distance L as a functional of the distribution functions at the origin. We thus have a system of coupled equations for the approximate distribution functions after a distance L, which is valid to second order in the interaction and has the form

$$f_{\alpha,L}(E) = F[f_{\alpha,0}, f_{\bar{\alpha},0}] + O(V^3)\,. \tag{19}$$

Iterating this, we obtain a recursive relation

$$f_{\alpha,nL}(E) \approx F[f_{\alpha,(n-1)L}, f_{\bar{\alpha},(n-1)L}]\,, \tag{20}$$

where n is the iteration number. Thus we can calculate an approximation to the distribution functions at distances nL.

A typical result of this iterative procedure for three coupled ES's is shown in Fig. 5, where we show the evolution of the excess temperature of the inner ES, the outer ES and the additional relaxation channel (denoted with "bulk") as a function of the iteration number. For the numerical integration, we use a three points Simpson extrapolation rule. We see that the inner ES and the additional relaxation channel, which are initially at equilibrium both gain energy since their excess temperatures increase. This increase happens at the expense of the initially out of equilibrium outer ES, which loses energy during the relaxation processes and thereby its excess temperature decreases. All three converge towards the temperature $k_B T^{\infty,(3)}_{exc} = \{\mathcal{T}(1-\mathcal{T})\}^{1/2}|\mu_1 - \mu_2|/\pi$, expected from energy equi-partition. Inset (a) shows the distribution functions after 1 iteration and inset (b) after 54 iterations. Note in particular that all three distribution functions are found to converge towards Fermi functions (dashed (black) curves in inset (b) which are indistinguishable from the calculated distributions). While the chemical potentials of the equilibrated distribution functions of the inner ES and of the additional relaxation channel remain constant, the chemical potential of the equilibrated outer ES is given by $\mu_o^\infty = \mu_1 + \mathcal{T}(\mu_2 - \mu_1)$, in agreement with particle conservation within each ES and thereby current conservation. Finally, note that because the velocity is independent of energy, the relaxation process is independent of the chemical potentials of the inner ES and of the additional relaxation channel.

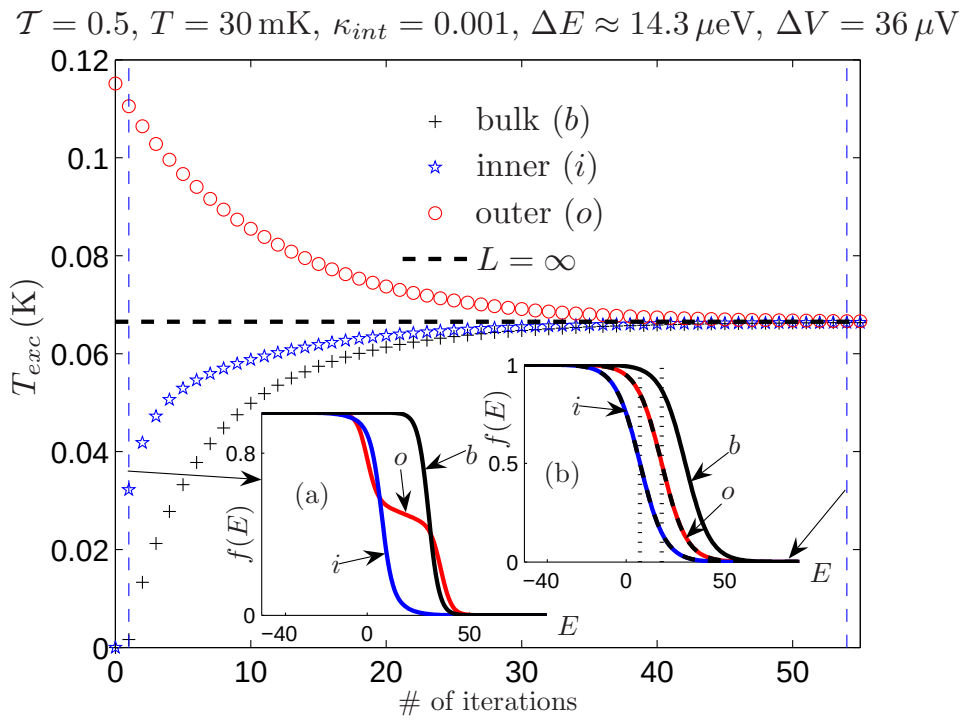

FIG. 5: (color online). Excess temperature as a function of the iteration number. Inset (a) shows the distribution functions after 1 iteration (i.e. the second order perturbation theory result) and inset (b) shows the distribution functions after 54 iterations where the edge states and the additional relaxation channel have relaxed into hot Fermi functions with the same temperature. The dashed vertical lines in inset (b) give the asymptotic values of the chemical potential of the two edge states ($\mu_i^\infty = \mu_i$ and μ_o^∞).

FITTING THE THEORY TO THE EXPERIMENT

A direct comparison of our theory with the experiment [7] is difficult because the absolute values of the interaction matrix elements among the ES's and between the inner ES and the bulk are unknown. Furthermore, we lack the knowledge of the proportionality constant α between the distance and the number of iterations. Nevertheless, using the matrix elements and the proportionality factor α as free parameters, we could fit all of the data for different voltage biases and lengths simultaneously, i.e. using the same parameters to fit different values of $\mu_2 - \mu_1$ and L. We find the best fit is obtained when the interaction strengths between the two outer ES's is about three times weaker than the interaction strength between the inner ES and the bulk excitations. The optimal value for the allowed energy transfer is found to be $\Delta E \approx 14.3\,\mu$eV. Following the literature [20], and taking the ES velocities to be between 10^4 and 10^5 m/s this leads to a lower bound of $0.5\,\mu$m for the momentum breaking length ℓ_p. This lower bound is smaller than the shortest measured propagation length of $0.8\,\mu$m and roughly one hundred times larger than the estimated magnetic length.

The length dependence of the excess temperature for the optimal parameters and for different values of $\Delta V = \mu_2 - \mu_1$, is shown in Fig. 6, where it is compared with the experiment. The thin dashed (red) curves give a least square exponential fit to the data. To obtain the excess temperature at an arbitrary distance x, we linearly interpolate the excess temperature from the numerical values obtained from the iteration procedure at distances $L\lfloor x/L \rfloor$ and $L(\lfloor x/L \rfloor + 1)$. This is how we obtain Fig. (3) of the main text.

Finally, in Fig. 7 we compare the cases with and without the extra relaxation channel, using the same optimal parameters as before. At small voltage biases, the data agrees well with the case where relaxation occurs only between the inner and the outer ES's, while for larger voltage biases it agrees at long distances only with the case where all three relaxation channels are effective. This clearly indicates that the energy is split among three and not two systems in the fully equilibrated limit.

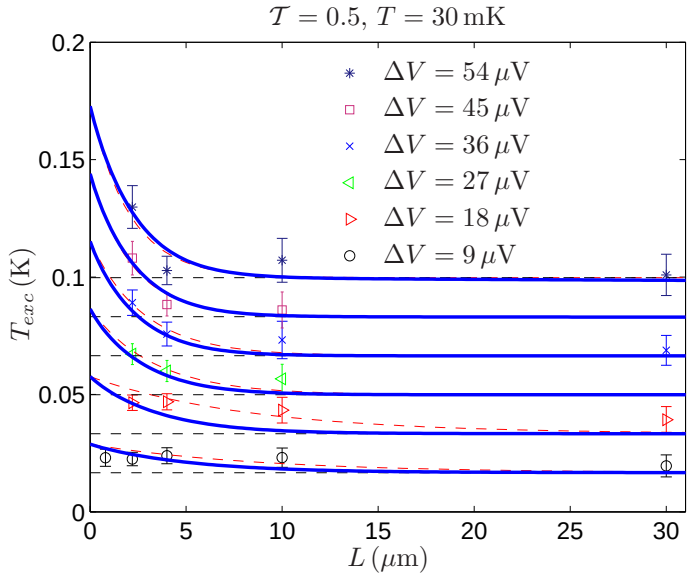

FIG. 6: (color online). Length dependence of the excess temperature of the outer edge state. Comparison between theory and experiment. Symbols with errorbars show the measurement results of [7]. The thin dashed (red) curves show a least square exponential fit to the data.

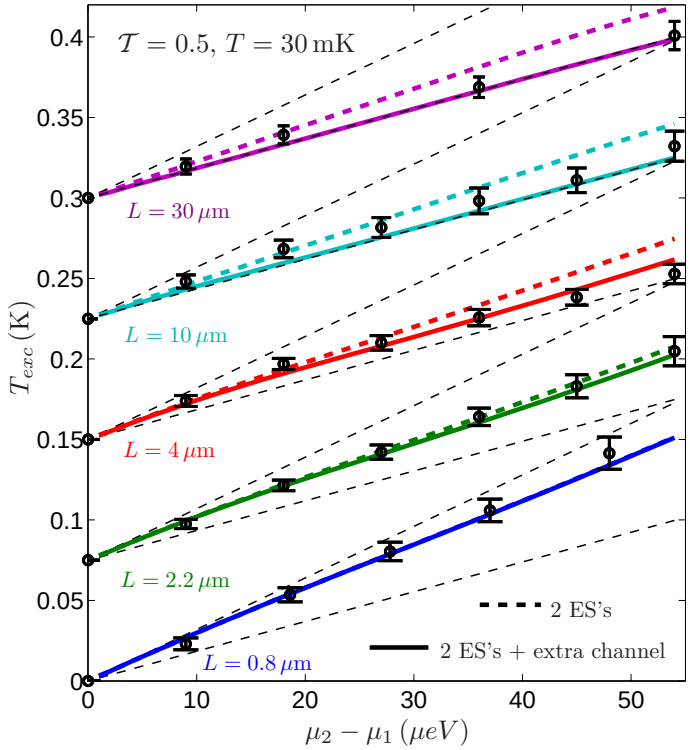

FIG. 7: (color online). Comparison between the models with (full thick curves) and without (dashed thick curves) additional relaxation channel. For small voltage biases $\mu_2 - \mu_1$ the data of [7] (black symbols with errorbars) is in good agreement with the model including relaxation among the inner and outer edge states only, while for larger voltages and long distances the agreement is markedly better with the model including an extra relaxation channel.